ICC
Iranian Chemical Communication
Original Research Article
Payame Noor University http://icc.journals.pnu.ac.ir

The computational study of adsorption of carbon monoxide on pristine and Ge-doped (6,0) zigzag models of BNNTs

Mahdi Rezaei Sameti*, Nina Alisafarzadeh

Department of Applied Chemistry, Faculty of Science, Malayer University, Malayer, 65174, Iran

Received: 16 January 2014, Accepted: 26 April 2014, Published: 26 April 2014

Abstract

The aim of this research is studying the effects of Ge-doped on CO adsorption on the outer and inner surfaces of (6, 0) zigzag model of boron nitride nanotube (BNNTs) by using DFT theory. For this purpose, eight models of CO adsorption on the surfaces of BNNTs are considered. At first step, all structures were optimized at B3LYP and 6-31G (d) standard base set and then the electronic structure, adsorption energy, HOMO - LUMO orbitals, gap energy, quantum molecular descriptors, and NQR parameters were determined. The bond lengths neighborhood sites of Ge-doped of BNNTs at all models were increased and the bond angles decreased. The small adsorption energy value and large interaction distance show that the adsorption of CO on BNNTs is weakly physical adsorption due to weak Van der Waals interaction. Our calculated results show that the adsorption of CO on the surface of undoped models is more favorable than Ge-doped models. The NQR parameters of the first layer in all the models are larger than those other layers.

Keywords: Boron nitride nanotube; density function theory; adsorption CO; Ge-doped; NQR.

Introduction

Since after the theoretically investigation of boron nitride nanotube in 1994, this nanotube was successfully synthesized experimentally in 1995 [1,2]. BNNTs have received great interest due to some essential properties such as their excellent chemical and thermal stabilities, mechanical properties, and potential

*Corresponding author: Mahdi Rezaei Sameti
Tel: +98 (851) 2355389, Fax: +98 (851) 2355389
E-mail: mrsameti@gmail.com

applications in chemical sensors and semiconductor properties with almost the same band gaps of 5.5 *eV* [3-9]. The slight positive charge of B and slight negative charge of N made the polarity and ionicity of the BNNTs larger than CNTs [10,11]. In the recent years, the detection of CO gas has been important for environmental researches because when the concentration of CO gas increases, it is dangerous for human body. For environmental safety and industrial control, several theoretical and experimental researches have reported CO adsorption on surfaces of novel materials [12-19].

Following our early researches [20-22], in the present work, we study the CO adsorption on the surfaces of undoped and Ge-doped BNNTs by using DFT theory because the previous works on the CO adsorption have indicated that the CO gas cannot be adsorbed on pure single-walled CNTs and BNNTs [23-26]. That is, we are motivated to do a theoretical study on the effect of Ge-doped on the adsorption of CO on the surface of BNNTs. Our study can help the researchers working on gas sensor or filter development.

Computational methods

In this project, the electronic structure, properties and NQR parameters of the CO adsorption on the (6,0) zigzag BNNTs are calculated by using the B3LYP level of theory and standard 6-31G (**d**) base set and using the Gaussian 03 set of programs [27-29]. At first step, we optimized eight (**a-h**) models of the CO adsorption on the outer and inner surface of undoped and Ge-doped of BNNTs. (Figure 1).

The adsorption energy (E_{ads}) of (CO) on the surfaces of undoped and Ge-doped BNNTs is calculated by Eqs. 1:

$$E_{ads} = E_{BNNTs-CO} - (E_{BNNTs} + E_{CO}) \quad (1)$$

Where $E_{BNNTs-CO,}$ E_{BNNTs} and E_{CO} are the electronic energy of the BNNTs–CO, BNNTs and CO respectively. The structures of HOMO and LUMO orbital and the gap energy between (Egap = E_{LUMO} - E_{HOMO}) are determined by the same level theory. From HOMO and LUMO energy, we calculate the quantum molecular descriptors involving electronic chemical potential (μ), global hardness (η), electrophilicity index (ω), global softness (S), The maximum amount of electronic charge, ΔN and electronegativity (χ) [30-33] of the nanotubes by using Eqs. (2-8).

$$\chi = -(I + A)/2 \quad (2)$$

$$\chi = -x \quad (3)$$

$$\mu = \chi^2/2\eta \quad (4)$$

$$\eta = (I - A)/2 \quad (5)$$

$$S = 1/2 \quad (6)$$

$$E_{gap} = E_{LUMO} - E_{HOMO} \quad (7)$$

$$\Delta N = \frac{-\chi}{\eta} \quad (8)$$

Where I ($-E_{HOMO}$) is the ionization potential and A ($-E_{LUMO}$) the electron affinity of the molecule. The nuclear quadruple coupling (C_Q) and asymmetry parameters (η_Q) are determined by Eqs. 9 and 10. The standard Q values for ^{14}N and ^{11}B are 20.44 and 40.59 *mb* respectively [34].

$$C_Q\ (MHZ) = e^2 Q q_{zz} h^{-1} \quad (9)$$

$$\eta_Q = |(q_{xx} - q_{yy})/q_{zz}| \quad (q_{zz} > q_{yy} > q_{xx}) \qquad 0 < \eta_Q < 1 \quad (10)$$

Result and discussion

Geometrical and structural parameters

Figures 1 and 2 indicate the (**a-h**) models of CO adsorption on the outer and inner surface of undoped and Ge-doped (6, 0) zigzag BNNTs. The calculated geometrical parameters, bonding energies, and electronic properties and quantum molecular descriptors are listed in Tables 1 and 2 respectively.

Table 1. Structural propertis of (a-h) models undoped and [Ge-doped] of (6, 0) zjgzag BNNTs. (Figures 1 and 2).In each column first value is for undoped and second value is for Ge-doped.

Bondlength(Å)	Pristine	Model(a)	Model(b)	Model(c)	Model(d)	Model(e)	Model(f)	Model(g)	Model(h)
B_{42} /Ge -N_{32}	1.46	1.46	1.46	1.48	1.48	1.47	1.48	1.46	1.46
B_{42}/Ge -N_{33}	[1.87]	[1.87]	[1.85]	[1.88]	[2.06]	[1.88]	[1.89]	[1.84]	[1.87]
B_{42}/Ge -N_{52}	1.46	1.46	1.46	1.48	1.48	1.47	1.48	1.46 1.85]	1.46
N_{32}-B_{22}	[1.87]	[1.82]	[1.85]	[1.88]	[2.06]	[1.88]	[1.89]	1.45	[1.86]
N_{32}-B_{41}	1.46	1.45	1.45	1.45	1.45	1.45	1.45	[1.81]	1.45
N_{33}-B_{23}	[1.82]	[1.82]	[1.81]	[1.83]	[1.89]	[1.83]	[1.82]	1.45	[1.82]
N_{33}-B_{43}	1.46	1.45	1.45	1.46	1.46	1.45	1.46	[1.44]	1.45
N_{52}-B_{62}	[1.44]	[1.44]	[1.44]	[1.44]	[1.50]	[1.44]	[1.45]	1.46	[1.44]
N_{52}-B_{63}	1.46	1.46	1.46	1.48	1.48	1.47	1.48	[1.45]	1.46
	[1.45]	[1.45]	[1.45]	[1.46]	[1.50]	[1.46]	[1.46]	1.45	[1.45]
	1.46	1.45	1.45	1.46	1.46	1.45	1.46	[1.44]	1.45
	[1.44]	[1.44]	[1.44]	[1.44]	[1.50]	[1.44]	[1.45]	1.46	[1.44]
	1.46	1.46	1.46	1.48	1.48	1.47	1.48	[1.45]	1.46
	[1.45]	[1.45]	[1.45]	[1.46]	[1.50]	[1.46]	[1.46]	1.46	[1.45]
	1.46	1.46	1.46	1.46	1.46	1.48	1.47	[1.46]	1.46
	[1.45]	[1.45]	[1.46]	[1.46]	[1.44]	[1.46]	[1.46]	1.46	[1.45]
	1.46	1.46	1.46	1.46	1.46	1.48	1.47	[1.46]	1.46
	[1.45]	[1.45]	[1.46]	[1.46]	[1.44]	[1.46]	[1.46]		[1.45]

Bond angel(0)									
N_{33}-B_{42}/Ge-N_{32}	117[101]	118 [101]	118 [103]	120 [105]	119 [71]	119 [105]	119 [105]	118 [103]	118 [101]
N_{33}-B_{42}/Ge-N_{52}	120 [104]	120 [104]	120 [106]	119 [103]	119 [89]	119 [103]	119 [102]	120 [106]	120 [104]
N_{32}-B_{42}/Ge-N_{52}	120 [104]	120 [104]	120 [106]	119 [103]	119 [89]	119 [103]	119 [102]	120 [106]	120 [104]
B_{42}/Ge-N_{32}-B_{22}	119 [109]	120 [104]	120 [106]	119 [103]	117[112] 111[126]	119 [103]	119 [102]	120 [106]	118 [109] 111 [118]
B_{42}/Ge-N_{32}-B_{41}	112 [118]								
B_{42}/Ge-N_{33}-B_{23}	119 [109]	118 [109]	118 [109]	117 [108]	117[112] 111[126]	117 [108]	117 [108]	118 [109]	118 [109] 111 [118]
B_{42}/Ge-N_{33}-B_{43}	112 [118]								
B_{42}/Ge-N_{52}-B_{63}	119 [120]	111 [118]	111 [117]	111 [120]	118[124] 118[124]	113 [120]	113 [120]	111 [117]	118 [120] 118 [120]
B_{42}/Ge-N_{52}-B_{62}	119 [120]								
		118 [109]	118 [109]	117 [108]		117 [108]	117 [108]	118 [109]	
		111 [118]	111 [117]	111 [120]		113 [120]	113 [120]	111 [117]	
		118 [120]	118 [119]	118 [120]		188 [120]	188 [120]	118 [119]	
		118 [120]	118 [119]	118 [120]		118 [120]	118 [120]	118 [119]	

Geometrical parameters show that the bond length B_{42}–N_{32}, B_{42}–N_{33} and B_{42}–N_{52} of all Ge-doped models increase from 1.46 Å to 1.87 Å. By C O adsorption, the bond length of B_{42}-N_{32} and B_{42}–N_{33} of (d) model of Ge-doped inrease from 1.48 Å to 2.06 Å, and on the other models, the bond length slightly increases. The bond angles of <N_{33}–B_{42}/Ge-N_{32}, <N_{33}–B_{42}/Ge–N_{52} and <N_{32}–B_{42}/Ge–N_{52} of (d) model of Ge-doped decrease significantly from 119^o to 71^o, 89^o and 89^o respectively. These results lead to change in hybridization from SP_2 to SP_3 at the B–N bonds. In addition, the bond angles close to CO regions indicate some difference in comparison to the pristine model reflecting some structural deformations. The calculated adsorption energy of all models is given in Table 2.

The results show that the CO adsorption energy is exothermic in all of the models. On the other hand, the adsorption energy of (a) undoped model is -15.24 Kcal/mol and, therefore, this model is more favourable than those other models. With doping of Ge, the adsorption energy of all the models decreases from undoped models. The small adsorption energy values and large interaction distance from the CO with BNNTs complex indicated

that CO adsorption is weakly physical due to the weak Van der Waals interaction between the nanotube and CO.

Table 2. Quantum molecular descriptors of (**a-h**) models of undoped and Ge-doped of BNNTs (Figure 1)

	Adsorption CO on undoped BNNTS								
	pristine	**Model (a)**	**Model (b)**	**Model (c)**	**Model (d)**	**Model (e)**	**Model (f)**	**Model (g)**	**Model (h)**
E(ads)/Kcal/mol	-	-15.24	-11.97	-14.69	-14.69	-14.97	-14.97	-11.97	-11.97
E(HOMO)/eV	-6.34	-6.69	-6.67	-6.72	-6.72	-6.70	-6.70	-6.67	-6.66
E(LUMO)/eV	-1.66	-1.80	-1.77	-1.82	-1.82	-1.81	-1.85	-1.77	-1.77
E(gap)/eV	4.68	4.89	4.90	4.90	4.90	4.89	4.85	4.90	4.89
η/ev	2.34	2.44	2.45	2.45	2.45	2.44	2.44	2.45	2.44
S/(eV)$^{-1}$	0.21	0.20	0.20	0.20	0.20	0.20	0.21	0.20	0.20
μ/eV	-4	-4.24	-4.22	-4.27	-4.27	-4.25	-4.27	-4.22	-4.21
X/eV	4	4.24	4.22	4.27	4.27	4.25	4.27	4.22	4.21
ω/eV	3.42	3.69	3.63	3.72	3.72	3.69	3.76	3.63	3.62
ΔN	1.71	1.74	1.72	1.74	1.74	1.74	1.76	1.72	1.72
	Adsorption CO on Ge-doped BNNTS								
E(ads)/Kcal/mol	-	-0.27	-0.54	-2.45	-3.54	-2.45	-2.45	-0.54	-0.27
E(HOMO)/eV	-5.96	-5.96	-5.21	-5.93	-5.93	-5.93	-5.98	-5.21	-5.96
E(LUMO)/eV	-1.69	-1.68	-1.80	-1.70	-1.70	-1.70	-1.74	-1.80	-1.67
E(gap)/eV	4.27	4.28	3.41	4.23	4.23	4.23	4.28	3.41	4.29
η/eV	2.13	2.14	1.70	2.11	2.11	2.11	2.14	1.70	2.14
S/(eV)$^{-1}$	0.23	0.23	0.29	0.24	0.24	0.24	0.23	0.29	0.23
μ/eV	-3.82	-3.82	-3.50	-3.81	-3.81	-3.81	-3.86	-3.50	-3.81
X/eV	3.82	3.82	3.50	3.81	3.81	3.81	3.86	3.50	3.81
ω/eV	3.42	3.41	3.59	3.44	3.44	3.44	3.48	3.59	3.38
ΔN	179	1.78	2.06	1.81	1.81	1.81	0.90	2.06	1.78

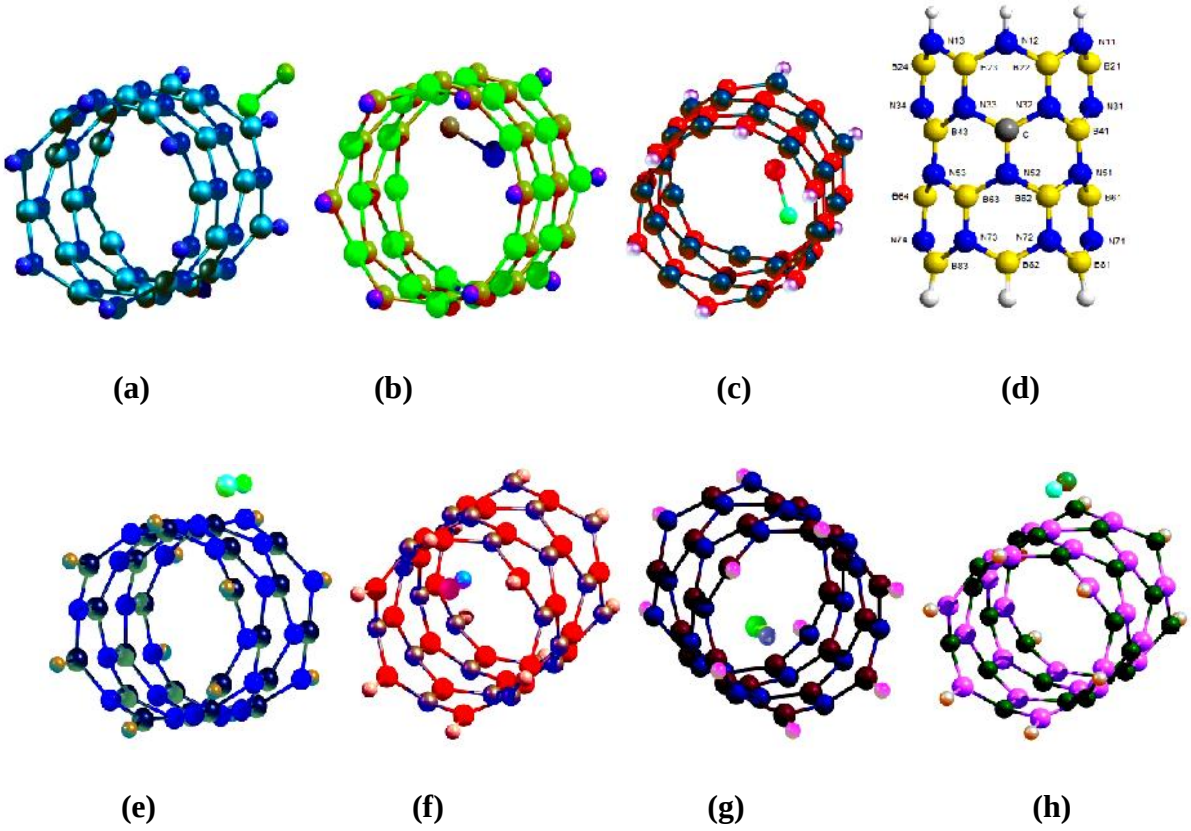

Figure 1. 2D views of CO adsorption on the (6, 0) zigzag model of BNNTs For Models (a-h):

(a) Vertical adsorption of CO gas on the outer surface of BNNTs *via* oxygen head

(b) Vertical adsorption of CO gas on the inner surface of BNNTs *via* oxygen head

(c) Vertical adsorption of CO gas on the outer surface of BNNTs *via* carbon head

(d) Vertical adsorption of CO gas on the inner surface of BNNTs *via* carbon head

(e) Parallel adsorption of CO gas on the outer surface of BNNTs *via* oxygen head

(f) Parallel adsorption of CO gas on the inner surface of BNNTs *via* oxygen head

(g) Parallel adsorption of CO gas on the outer surface of BNNTs *via* carbon head

(h) Parallel adsorption of CO gas on the inner surface of BNNTs *via* carbon head

Molecular orbital (MO) and Quantum molecular descriptor

Figures 2 and 3 display the calculated structure of HOMO and LUMO orbital of CO adsorption on the surfaces of considered (a-h) undoped and Ge-doped models BNNTs.

The electronic charge density of HOMO orbital in (c, d, e, and f) models is located at the first layers of nanotube (Figure 2). However, the electronic charge densities of LUMO orbital in all models are located on B sites of nanotubes. The gap energy between HOMO and LUMO orbital (E_{gap}) of the nanotube can evaluate the reactivity of the chemical adsorption and electronic property of two species. Therefore, the E_{gap} of the in-

trinsic undoped and Ge-doped (6, 0) BNNTs are found to be 4.68 and 4.27 eV respectively (see Table 2). The E_{gap} on (**b**, **g**) Ge-doped models of BNNTs decreases to 3.41 eV. The decrease of gap energy can prove that the chemical activity of complex BNNTs/CO has been increased and hence the chemical stability of the nanotube will be decreased. The quantum molecular descriptors of the nanotubes are calculated by Eqs (2-8) and the results are given in Table 2. The global hardness (η) is defined as a resistance to deformation in the presence of an electric field that can be increased with stability and can be decreased in reactivity of the species. The average of global hardness for (**a-h**) undoped models of BNNTs is 2.40 eV and for (**a-h**) Ge-doped models of BNNTs are 1.92 eV. The results indicate that the global hardness (η) of (**b**, **g**) Ge-doped models are smaller than those other models. However, the global softness (S), electronegativity (χ) of (**b**, **g**) models are larger than other models. These results demonstrate that electrons will flow from a definite occupied orbital in a Ge atom of BNNTs and will go into a definite empty orbit in a CO. The electrophilicity index (ω) of (a-h) Ge-doped models is lower than all undoped models. Therefore, maximum flow of electron takes place from the Ge atom (as donor atom) to nanotube (as acceptor species) and supplies the structural stability and reactivity of nanotube complex.

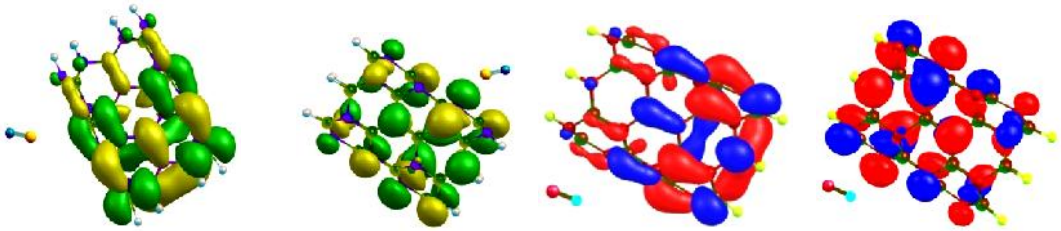

(a1) **(a2)** **(b1)** **(b2)**

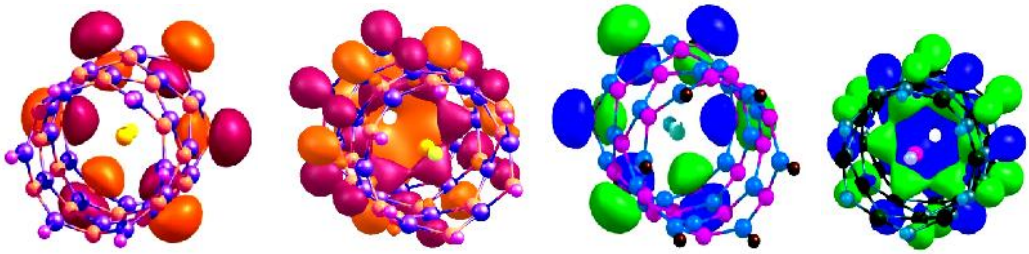

(c1) **(c2)** **(d1)** **(d2)**

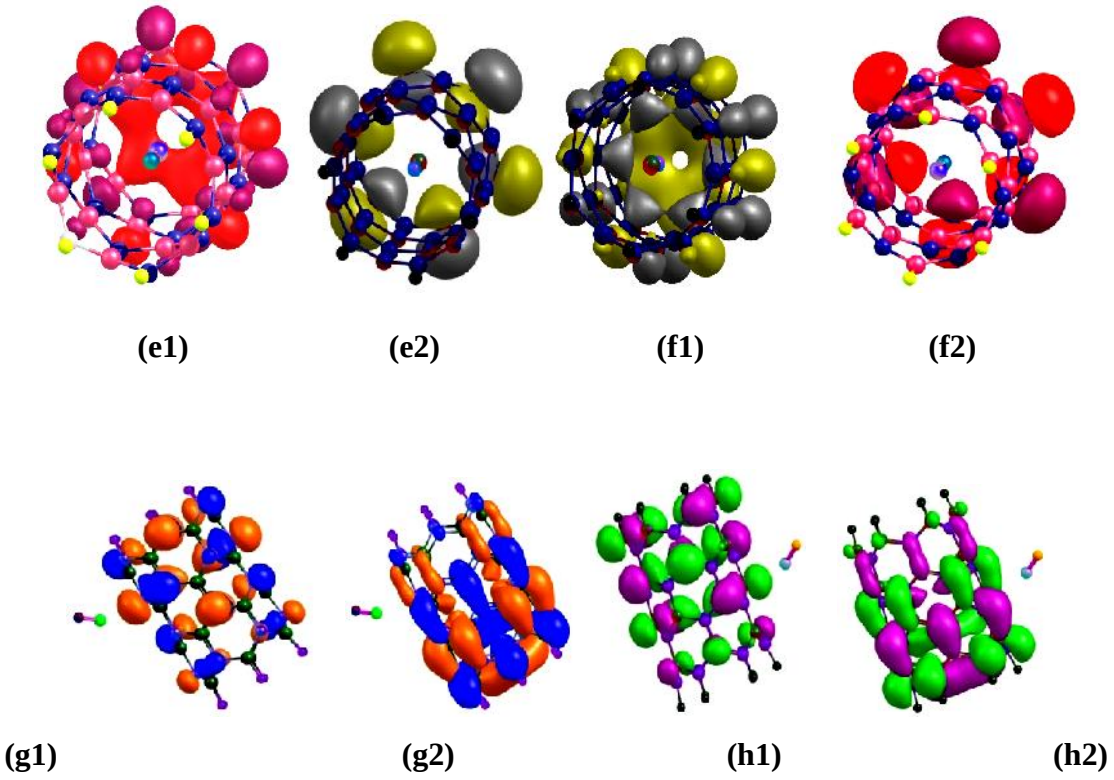

Figure 2. The HOMO and LUMO structures of CO adsorption on the (a-h) undoped of (6, 0) zigzag model of BNNTs (See Figure 1), index 1 is used for HOMO and index 2 for LUMO orbital.

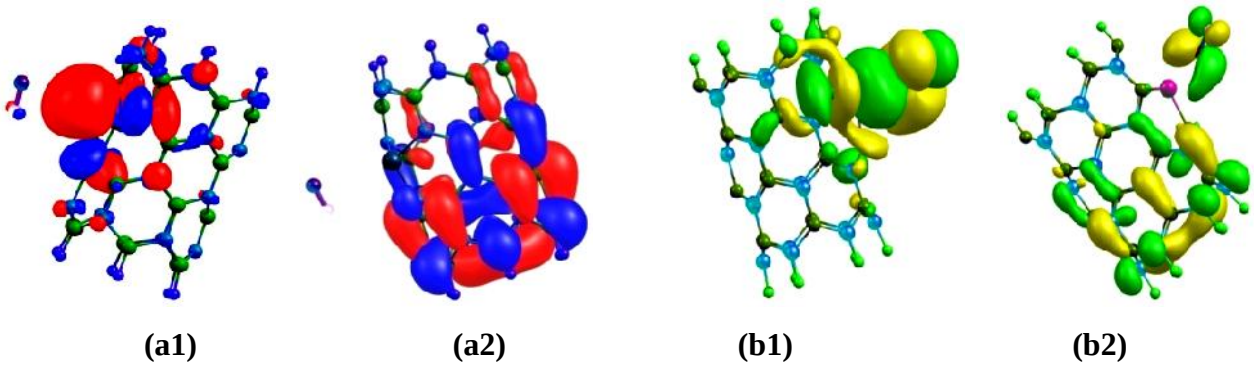

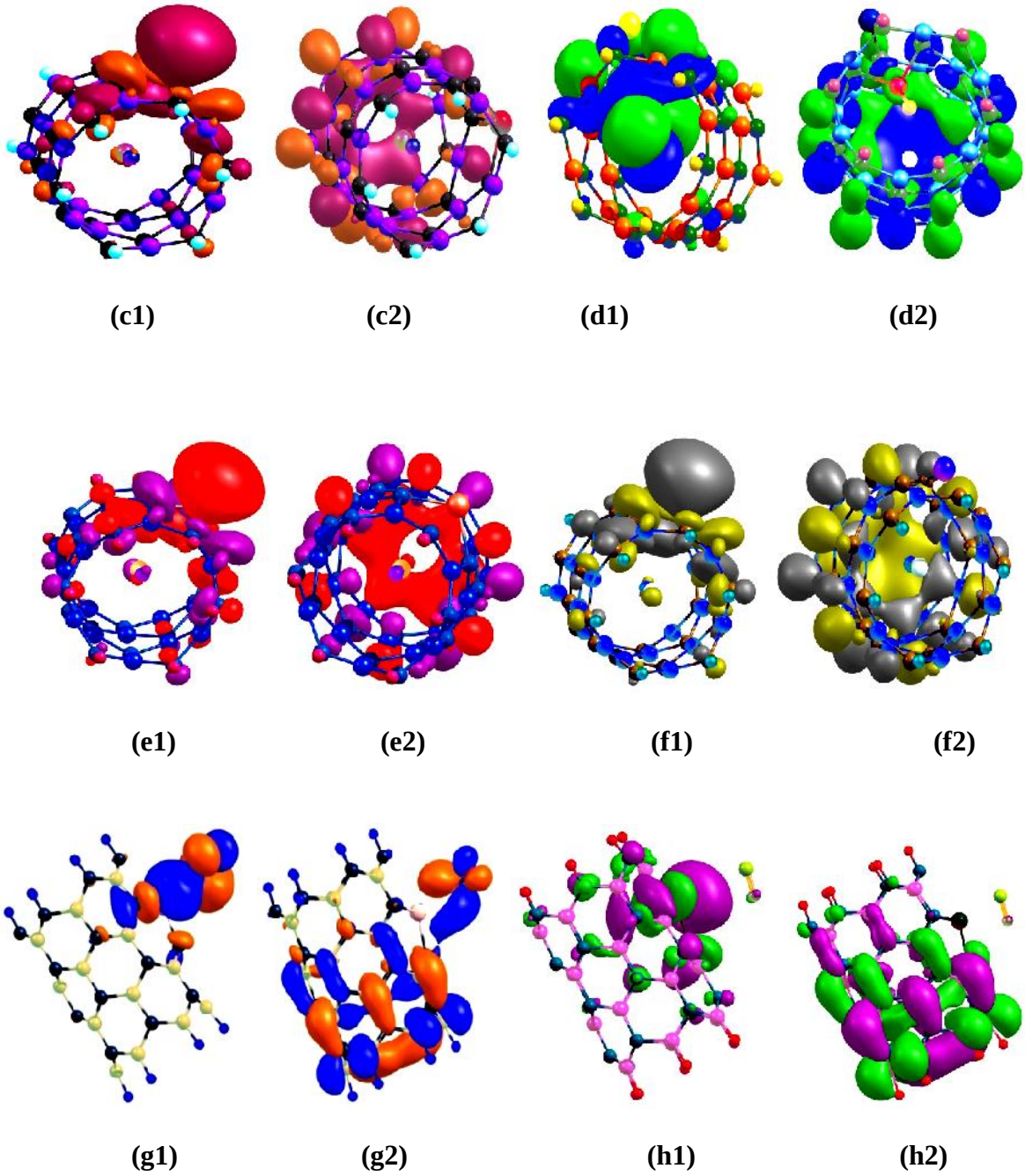

Figure 3. The HOMO and LUMO structures of CO adsorption on the (a-h) Ge-doped of (6, 0) zigzag model of BNNTs (See Figure 1), index 1 is used for HOMO and index 2 for LUMO orbital.

NQR Parameters

The NQR parameters for all models at the sites of various ^{11}B and ^{14}N atoms are calculated by Eqs. 9-10 and results are summarized in Tables 3 and 4. The results reveal that the calculated NQR parameters are not similar for various nuclei; hence, the electrostatic environment of the BNNT is not

equivalent throughout the lengths of the nanotube models.

The results of Table 3 reveal that the asymmetry parameters (η_Q) for B sites of the first layers of (**a-h**) undoped models are almost constant. However, the η_Q values for B nuclei on other layers are slightly changed. The η_Q values for N nuclei (Table 3) of the second layer in all the models except for (c and d) models are significantly increased.

Table 3. NQR parameters of CO adsorption at different (**a-h**) models (Figure 1) undoped of (6, 0) zigzag BNNTs

	Pristine		Model(a)		Model(b)		Model(c)		Model(d)		Model(e)		Model(f)		Model(g)		Model(h)	
	NQR parameters B-atom																	
	η	CQ	η	CQ	η	CQ	η	CQ	η	CQ	η	CQ	η	CQ	η	CQ	η	CQ
Layer 1	0.30	3.96	0.11	2.53	0.11	2.54	0.08	2.47	0.08	2.47	0.11	2.54	0.09	2.49	0.11	2.53	0.11	2.53
Layer 2	0.09	2.60	0.07	2.59	0.07	2.58	0.11	2.69	0.11	2.69	0.05	2.55	0.11	2.69	0.07	2.58	0.07	2.60
Layer 3	0.07	2.54	0.09	2.66	0.09	2.66	0.09	2.67	0.09	2.67	0.13	2.76	0.10	2.68	0.09	2.66	0.09	2.66
Layer 4	0.11	2.47	0.28	3.92	0.28	3.92	0.28	3.92	0.28	3.93	0.29	3.93	0.28	3.93	0.28	3.92	0.28	3.92
	NQR parameters N-atom																	
	η	CQ	η	CQ	η	CQ	η	CQ	η	CQ	η	CQ	η	CQ	η	CQ	η	CQ
Layer 1	0.34	1.82	0.84	4.17	0.84	4.17	0.65	4.52	0.65	4.52	0.83	4.23	0.79	4.31	0.84	4.17	0.84	4.18
Layer 2	0.03	1.92	0.07	1.92	0.07	1.92	0.11	2.11	0.11	2.11	0.25	2.09	0.37	2.01	0.07	1.91	0.07	1.91
Layer 3	0.04	2.05	0.09	1.76	0.09	1.77	0.08	1.86	0.08	1.86	0.09	2.03	0.01	2.08	0.09	1.77	0.09	1.76
Layer 4	0.69	4.67	0.45	1.59	0.45	1.59	0.45	1.57	0.45	1.57	0.42	1.67	0.46	1.56	0.44	1.59	0.44	1.58

The results in Table 4 show that the η_Q values of B nuclei of first layers for all (**a-h**) Ge-doped models are constant and the other layers slightly change. The nuclear quadrupole coupling (C_Q) values for B nuclei of the first layer in all models are larger than those

other layers. It is notable that the C_Q values for N nuclei of the first layers of (**a**, **b**, **g**, and **h**) undoped models are smaller than other models. This trend is in agreement with the changes in the structural properties and quantum descriptors of the BNNTs/CO complex.

Table 4. NQR parameters of CO adsorption at different (**a-h**) models (Figure 2) Ge-doped of (6, 0) zigzag BNNTs

	Pristine		Model(a)		Model(b)		Model(c)		Model(d)		Model(e)		Model(f)		Model(g)		Model(h)	
NQR parameters B-atom																		
	η	CQ	η	CQ	η	CQ	η	CQ	η	CQ	η	CQ	η	CQ	η	CQ	η	CQ
Layer 1	0.11	2.52	0.11	2.52	0.11	2.53	0.12	2.54	0.20	2.80	0.12	2.55	0.10	2.50	0.12	2.53	0.11	2.52
Layer 2	0.07	2.52	0.07	2.53	0.06	2.52	0.05	2.49	0.22	2.93	0.05	2.49	0.11	2.63	0.06	2.52	0.07	2.53
Layer 3	0.10	2.66	0.10	2.66	0.09	2.68	0.13	2.75	0.10	2.67	0.13	2.75	0.10	2.66	0.12	2.68	0.10	2.66
Layer 4	0.27	3.91	0.28	3.91	0.28	3.92	0.29	3.93	0.28	3.90	0.29	3.93	0.28	3.91	0.28	3.92	0.28	3.91
NQR parameters N-atom																		
	η	CQ	η	CQ	η	CQ	η	CQ	η	CQ	η	CQ	η	CQ	η	CQ	η	CQ
Layer 1	0.83	4.13	0.83	4.22	0.83	4.22	0.82	4.26	0.77	4.47	0.72	4.26	0.78	4.34	0.83	4.21	0.83	4.22
Layer 2	0.37	1.97	0.37	1.97	0.36	2.02	0.45	2.18	0.32	2.36	0.55	2.18	0.51	2.07	0.36	2.02	0.37	1.96
Layer 3	0.17	2.12	0.18	2.11	0.17	2.12	0.17	2.32	0.12	2.25	0.17	2.32	0.13	2.42	0.17	2.12	0.18	2.11
Layer 4	0.51	1.54	0.51	1.54	0.51	1.54	0.48	1.61	0.50	1.62	0.48	1.62	0.51	1.51	0.51	1.54	0.51	1.54

Conclusion

In this research, we performed density functional theory (DFT) to calculate the structural parameters, quantum descriptors and NQR parameters to investigate the effects of Ge-doped on CO adsorption on BNNTs. The bond lengths of (**a-h**) Ge-doped models increase and the bond angles decrease because of the change in the hybridization of atoms to SP_3 hybridization. The computational results

show that the interactions between CO and BNNTs in all models are also physorption and CO adsorption of the undoped model is more favorable than a Ge - doped model. The NQR parameters of the first and second layers of all models are significantly changed.

Acknowledgments

The authors thank the computational Centre of Malayer University for supporting this project.

References

[1] A. Rubio, J.L. Corkill, M.L. Cohen, *Phys. Rev. B*, **1994**, *46*, 5081-5084.

[2] N.G. Chopra, R.J. Luyken, K. Cherry, V.H. Crespi, M.L. Cohen, S.G. Louie, A. Zettl, *Science* **1995**, *269* , 966-967.

[3] J. Yuan, K.M. Liew, *Carbon.*, **2011**, *49*, 677–683.

[4] J.F. Jia, H.S. Wu, H. Jiao, *Physica B.*, **2006**, *381*, 90–95.

[5] L. Li, C.P. Li, Y. Chen, *Physica E*., **2008**, *40*, 2513-2516.

[6] C.Y. Zhi, Angew. *Chem. Int. Ed.*, **2005**, 44, 7929-7932.

[7] G. Wen, T. Zhang, X.X. Huang, B. Zhong, X. D. Zhang and H.M. Yu, *Scrip. Mater*., **2010**,62, 25-29.

[8] X. Blase, A. Rubio, S.G. Louie, M.L. Cohen, Euro. Phys. Let., **1994,** 28, 335-340.

[9] D. Goldberg, Y. Bando, M. Milton, *Physica B.*, **2002**, *323*, 60-66.

[10] M. Mirzaei, A. Nouri, *J. Mole. Struct. (THEOCHEM).*, **2010**, *942*, 83–87

[11] A. Soltani, S. Ghafouri Raz, V. Juvenile Rezaei, A. Dehno Khalaji, M. Savar, *Appl. Surf. Science,* **2012**, *263*, 619-625.

[12] R. Ma, Y. Bando, H. Zhu, T. Sato, C. Xu, D. Wu, *J. Am. Chem. Soc*., **2002**, *124*, 7672-7673.

[13] J.X. Zhao, B. Gao, Q.H. Cai, X.G. Wang, X.Z. Wang, *Theor. Chem. Acc*., **2011**, *129*, 85-88.

[14] A. Ahmadi Peyghan, M.T. Baei, M. Moghimi, S. Hashemian, *J. Clust. SCI,*. **2013**, *24*, 341-347.

[15] J. Beheshtian, H. Behzadi, M.D. Esrafili, B.B. Shirvani, N.L. Hadipour, *Struct. Chem*,. **2010**, *21*, 903-908.

[16] R.J. Chen, H.C. Choi, S. Bangsaruntip, E. Yenilmez,X.Tang,Q.Wang, T.L. Chang, H. Dai, *J. Am. Chem. Soc.*, **2004**, 126, 1563-1568.

[17] A. Ahmadi, M. Kamfiroozi, J. Beheshtian, N. L. Hadipour, *Struct. Chem.* **2011**, 22, 1261-1265.

[18] J. Yu, K. Huang, J. Tang, *Physica E*., **2008**, *41*, 181-184.

[19] S. Xu, C. Wang, Y. Cui, *Struct. Chem*., **2010**, *21*, 519-522.

[20] M. Rezaei-Sameti, *Physica E.*, **2010**, *43*, 588-592.

[21] M. Rezaei-Sameti, *J. Mol. Struc.(THEOCHEM).*, **2008**, *867*, 122-130.

[22] M. Rezaei-Sameti, *Physica B.*, **2012**, *407*, 22-26.

[23] R. Mota, S.B. Fagan, A. Fazzio, *Surf Sci.*, **2007**, *601*, 4102-4104.

[24] K. Azizi, S.M. Hashemianzadeh, S. Bahramifar, *Curr. Appl. Phys.*, **2011**, *11*, 776-782.

[25] R. Wang, D. Zhang, W. Sun, Z. Han, C. Liu C, *J. Mol. Struct. THEOCHEM*, **2007**, *806*, 93-97.

[26] R.J. Baierle, T.M. Schmidt, A. Fazzio, *Solid State Commun*., **2007**, *142*,49–53.

[27] C. Lee, W. Yang, R.G. Parr, *Phys. Rev. B.*, **1988**, *37*, 785-789.

[28] M.J. Frisch, *et al.*, GAUSSIAN 03, **2003**.

[29] R. Ditchfield, W.J. Hehre, J. A. Pople, *J. Chem. Phys.*, **1972**, *54*, 724-728.

[30] M.T. Baei, M. Moghimi, P. Torabi, A.Varasteh Moradi, *Comput. Theor. Chem*., **2011**, *972*, 14-19

[31] P.K. Chattaraj, U. Sarkar, D. R. Roy, ***Chem. Rev.*, 2006, *106*, 2065-2091.**

[32] K.K. Hazarika, N.C. Baruah, R. C. Deka, *Struct. Chem*., **2009**, *20*, 1079-1085.

[33] R.G. Parr, L. Szentpaly, S. Liu, *J. Am. Chem. Soc*., **1999,** *121*, 1922-1924.

[34] P. Pyykkö, *Mol. Phys*., **2001**, *99*, 1617-1629.